

# Spatiotemporal intermittency in the critical dynamics of dc-driven two-dimensional frustrated Josephson arrays

Italo F. Marino<sup>1,2</sup> and Manuel G. Velarde<sup>1</sup>

<sup>1</sup>*Instituto Pluridisciplinar, Universidad Complutense, Paseo Juan XXIII, No. 1, Madrid 28040, Spain*

<sup>2</sup>*Science Department, Saint Louis University, Madrid Campus, Avda. del Valle 28, Madrid 28003, Spain*

(Received 5 April 2001; published 19 October 2001)

We report the numerical observation of spatiotemporal intermittency in the critical dynamics of two-dimensional frustrated underdamped dc-driven Josephson junction arrays. This intermittency is due to the hopping of the system among the different subcritical metastable states, which are characterized by domain walls separating regions with the symmetry of the ground state. Turbulentlike domains correspond to the regions surrounding the nucleation and decay of these domain walls, or equivalently, to the regions where vortex motion takes place. This intermittency is further signaled by the observation of  $1/f$  noise in the high-frequency tail of the power spectrum of the voltage fluctuations, and by the scaling of the characteristic time scale for front propagation with the current. A study of the ground and metastable states of the system is also presented.

DOI: 10.1103/PhysRevB.64.184513

PACS number(s): 74.50.+r, 03.75.Fi, 05.30.Jp, 32.80.Pj

## I. INTRODUCTION

Spatiotemporal intermittency was first proposed by Pomeau when considering that turbulence may originate via a subcritical bifurcation with front formation.<sup>1</sup> This phenomenon is characterized by the presence of laminar and turbulent domains, and intermittent fluctuations in time, and it can be understood using tools borrowed from the theory of phase transitions,<sup>2</sup> although no universality has yet been shown.

It has been observed in the numerical simulations of a variety of discrete spatially extended systems, in particular in coupled-map lattices,<sup>3,4</sup> and recently it has been observed in the numerical simulations of an array of globally coupled ac-driven Josephson junctions.<sup>5</sup> In the latter, the global coupling and the intermittent behavior of the single junctions prove to be essential for its observation.

In this paper we show the presence of spatiotemporal intermittency in the critical dynamics of a numerical model of a two-dimensional underdamped frustrated array of Josephson junctions, driven by a uniform dc current. The chaotic nature of these oscillations was first observed by Falo *et al.*,<sup>6</sup> who nevertheless attempted to explain it in terms of the Frenkel-Kontorova model. The dynamics of this system has also been subject to study at high voltages, in the dc case in Refs. 7,8, and in the ac case in Ref. 9. Our result differs from that of Xie and Cerdeira<sup>5</sup> in that in our case the junctions in the uncoupled case are not chaotic (since they can be chaotic only in the presence of an ac driving), which implies that the fluctuations (or chaotic oscillations) arise due to a collective instability, and in the fact that we use only nearest-neighbor coupling, which allows the possibility of the appearance of spatial structures. We find that this intermittency is due to the hopping of the system among the different subcritical metastable states (which are all unstable above the critical current), a result which somewhat resembles what has been observed in the case of a single junction, where the hopping occurs among the different unstable periodic solutions.<sup>10,11</sup> This result can as well be related with the generic mechanism

for spatiotemporal intermittency proposed by Argentina and Coulet,<sup>12</sup> according to which the intermittency is due to the bistability of their system between an oscillatory state and a stationary state.

This hopping occurs through the nucleation and decay of domain walls separating regions with the symmetries of the ground state, a process seemingly stochastic, and which requires a local motion of vortices near the domain walls which are being created or destroyed, giving rise to local chaotic voltage oscillations. This local vortex motion defines a “turbulentlike” region, which propagates through an “infection” process, a feature of spatiotemporal intermittency. This spatiotemporal intermittency is further signaled by the appearance of  $1/f$  noise in the high-frequency tail of the power spectrum of the average voltage oscillations in the system. At lower frequencies, this scaling relationship is destroyed by the presence of the Josephson and plasma frequencies. In addition, the time scale characteristic of front propagation displays a scaling relationship with the current, which is another signature of the critical nature of the oscillations.

We find as well that for  $f=1/2$  the fluctuations are two dimensional. This does not allow an understanding of the situation, given that now it is impossible for us to identify the defects and metastable states. For  $f=1/3$  and  $f=2/5$  we find that the fluctuations are quasi-one-dimensional.

The paper is divided as follows. In Sec. II we discuss the mathematical model on which our study is based. In Sec. III we present a study of the ground states of the system as a function of the injected current. In Sec. IV we discuss the metastable states of the system. In Sec. V we study the critical fluctuations of the system, discussing the dynamics of the domain walls, and the nature of the instability giving rise to the fluctuations, and finally in Sec. VI we present some conclusions.

## II. THE MODEL

We consider a square array of underdamped Josephson junctions with parallel shunt resistance and capacitance  $R$

and  $C$ , respectively,  $f (= p/q, p$  and  $q$  being relatively prime integers) magnetic flux quanta piercing each plaquette, applied perpendicularly to the array, a critical current per junction  $i_0$ , a uniformly injected dc current  $i_{dc}$  along a direction taken as horizontal, and periodic boundary conditions with period  $q$  along the vertical direction. We shall also set the horizontal length of the array to be equal to an integer multiple of  $q$ . As we shall verify below, these boundary conditions will determine that the dynamics be quasi-one-dimensional (save for the case in which  $f=1/2$ ), being this dimension the horizontal dimension, as there is no symmetry-breaking perturbation along the vertical direction.

The dynamical variables are the gauge-invariant phase differences  $\theta_{ij} = \theta_i - \theta_j - A_{ij}$ , where  $\theta_i$  is the superconducting phase on the  $i$ th site on the array, and  $A_{ij}$  is equal to  $2e/(\hbar c)$  times the line integral of the vector potential from  $i$  to  $j$ . The equations of motion express the conservation of the current at each site  $i$  on the array

$$\sum_{\langle j \rangle} \left[ \beta \frac{d^2}{dt^2} \theta_{ij} + \frac{d}{dt} \theta_{ij} + \sin(\theta_{ij}) \right] = 0, \quad (2.1)$$

the sum being over nearest neighbors. In this equation, quantities are expressed in dimensionless units: time is measured in units of  $\tau_0 = \hbar/(2ei_0R)$ , current is measured in units of  $i_0$ , and  $\beta = (2ei_0R^2C)/\hbar$  is the MacCumber dimensionless number.<sup>13</sup> The first term represents the displacement current, the second the normal current, due to the tunneling of quasiparticles, and the last one, the supercurrent. A gauge which is convenient to use is the Landau gauge, according to which  $A_{ij} = 2\pi fn$ , wherein both  $i$  and  $j$  lie on a vertical bond on the  $n$ th column, and zero on horizontal bonds. The current  $I$  (which is the dc current measured in units of  $i_0$ ) is injected at each site at the left boundary (the equation for current conservation continues to hold, with the expression for the current on the left junction replaced by the dc current), and removed at the right boundary.

The phase configuration of the system can as well be visualized through its vortex configuration. At each plaquette of the system, we define the so-called vorticity  $n_v$  (in degenerate albeit common terminology, as it actually corresponds to the circulation) through the sum of the gauge-invariant phase differences around the plaquette,

$$\sum_P (\theta_i - \theta_j - A_{ij}) = 2\pi(n_v - f), \quad (2.2)$$

where the gauge-invariant phase differences are restricted to lie within the interval between  $\pm\pi$ . The average vorticity in the array is equal to  $f$ , which means that out of  $q$  plaquettes,  $p$  contain vortices (this terminology is also degenerate, as in this case there is no magnetic core associated with the ‘‘vortex’’) with  $n_v = 1$ .

This system possesses a critical current, below which the system settles into a state with vanishing normal and displacement currents, whereas above the critical current they are nonvanishing, and a dynamical situation ensues. Consequently, the equation satisfied by the gauge-invariant phase differences below the critical current in their steady state is

$$\sum_j \sin(\theta_i - \theta_j - A_{ij}) = 0. \quad (2.3)$$

This critical current, however, depends on the value of  $\beta$ .<sup>13</sup> In fact, as  $\beta$  increases, the critical current decreases. This is because when  $\beta$  is larger, the relative effect of dissipation becomes weaker, which eases the appearance of a finite voltage.

This last equation gives us the extrema of the function

$$H = -J \sum_{\langle ij \rangle} \cos(\theta_i - \theta_j - A_{ij}). \quad (2.4)$$

This function resembles the Hamiltonian, which is well defined only in the absence of normal and displacement currents, and which can be used to study the statistical mechanics of the system.<sup>13,14</sup> Although we can no longer interpret  $H$  as the Hamiltonian of the system, we can nevertheless interpret it as a Lyapunov functional, which tends to decrease under the application of an external current, for currents below the critical current. Notwithstanding, we shall continue to refer to this function as the ‘‘Hamiltonian.’’  $J$  is a parameter which depends on the temperature and the superconducting gap. Without loss of generality, we shall henceforth set it equal to unity.

The solutions of Eq. (2.3) play a fundamental role not only below the critical current, but also at the critical current, when they all become unstable, as we will see below. Below the critical current they are the metastable states of the system. Hence, we now turn to their study.

### III. GROUND STATES

The ground state is the state with lowest ‘‘energy,’’ defined according to Eq. (2.4). This state plays a fundamental role in the dynamics of this system, because it is the last state to become unstable under the application of an external current. Here we present a brief discussion of the ground states of the system, stressing their relationship to the injected current. A more thorough discussion will be published elsewhere.

These ground states were discussed by Halsey.<sup>15</sup> For this, he used the relationship that exists between this model and the charge model. Thus, he showed that for all values  $1/3 \leq f \leq 1/2$  the ground states were staircase states, oriented perpendicularly to one of the diagonals (of the  $q \times q$  unit cell). Assuming that the current runs along these staircases, he wrote down the expressions for the gauge-invariant phase differences for zero applied current

$$\tilde{\theta}(m) - \tilde{\theta}(m-1) = \pi fm + (\alpha/2) - \pi \text{nint}[fm + (\alpha/2\pi)], \quad (3.1)$$

where  $\text{nint}$  is the nearest integer function.  $\tilde{\theta}(m) - \tilde{\theta}(m-1)$  is the gauge-invariant phase difference along the  $m$ th staircase, and  $\alpha$  is a parameter to be determined by the minimization of the Hamiltonian.

Following Halsey’s prescription, we assume that the states have staircase symmetry, and thus in the presence of an applied current  $I$  all we need are the values of the  $q$  horizontal phases  $\theta_{Hk}$  and  $q$  vertical phases  $\theta_{Vk}$ , as shown in Fig. 1 (in

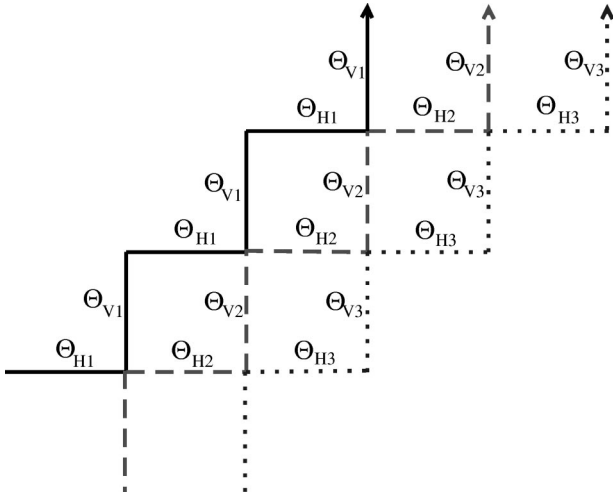


FIG. 1. Distribution of gauge-invariant phase differences for a staircase state with nonvanishing albeit small  $I$ . Only three staircases are shown, which are labeled by the index  $i=1,2,3$ . Notice that the horizontal (respectively vertical) phases are invariant under the translation along the staircase. For  $I=0$ ,  $\theta_{Vi} = \theta_{Hi}$ , so that the current is constant on each staircase, and runs in the direction indicated by the arrows (on some staircases the current runs in the opposite direction, so that the total current flowing is zero).

this case, the current is no longer constant along the staircase). We can then write down the expressions for the phases in terms of the expressions for the gauge-invariant phase differences for zero current,

$$\theta_{Hk} = \theta_{Hk}^{(0)} + a_k, \quad (3.2)$$

$$\theta_{Vk} = \theta_{Vk}^{(0)} + b_k, \quad (3.3)$$

where  $a_k$  and  $b_k$  vanish at zero current, and  $\theta_{Hk}^{(0)}$  and  $\theta_{Vk}^{(0)}$  are the horizontal and vertical gauge-invariant phase differences on the  $k$ th staircase for zero current.

The application of the equations for current conservation at each site on the array yields

$$\sin(\theta_{Hk}^{(0)} + a_k) - \sin(\theta_{Vk}^{(0)} + b_k) = \xi, \quad (3.4)$$

where  $\xi$  is a parameter independent of  $k$ , yet dependent on  $I$ . Likewise, the equation stating the relationship between the sum total of the phases around a plaquette and the vorticity can easily be written down in terms of the phases  $a_k$  and  $b_k$ , which leads to the relationship

$$a_k + b_k = \chi, \quad (3.5)$$

where  $\chi$ , as  $\xi$ , is a parameter independent of  $k$ , but dependent on  $I$ .

Imposing the boundary conditions through the relationship

$$\sum_{k=1}^q \sin(\theta_{Hk}^{(0)} + a_k) = qI, \quad (3.6)$$

and the minimization of the Hamiltonian with respect to variations of the parameters  $\xi$  and  $\chi$ , it is possible to obtain

$a_k$  and  $b_k$ . Moreover, in the limit of very small currents,  $I \ll 1$ , it is possible to write down explicit solutions, namely,

$$a_k = \frac{q \sin \frac{\pi}{2q}}{\lambda + q^2 \sin \frac{\pi}{2q}} [\lambda + q \sec(\theta_{Hk}^{(0)})] I, \quad (3.7)$$

$$b_k = \frac{q \sin \frac{\pi}{2q}}{\lambda + q^2 \sin \frac{\pi}{2q}} [\lambda - q \sec(\theta_{Hk}^{(0)})] I, \quad (3.8)$$

where

$$\lambda = \sum_{k=1}^q \sec(\theta_{Hk}^{(0)}). \quad (3.9)$$

We now turn to the study of the metastable states of the system.

#### IV. METASTABLE STATES

The metastable states are states in which the normal and displacement currents vanish. Consequently, they are solutions of Eq. (2.3). In this case it is no longer possible to write down analytical expressions, so we need to resort to numerical studies. For this we integrated the equations of motion using a fourth-order Runge-Kutta method, with time steps which varied between  $\Delta t = 0.01$  to  $\Delta t = 0.1$ . We then generated these states in two different manners. First, by running simulations starting with random initial conditions along the horizontal direction (so that the periodic boundary conditions along the vertical direction were respected), and secondly by starting off with ground states, then raising the current above the critical current, at which fluctuations occur, and by then lowering the current below the critical current. In all cases we studied, except those in which  $f=1/2$ , the states thus generated were quasi-one-dimensional, and were characterized by a random pattern of domain walls oriented perpendicularly to the current, separating regions with opposite symmetries of the ground states. In the case  $f=1/2$ , we obtained sometimes states which were disordered in the two dimensions, which suggests that in this case there is a transverse instability, as well as a longitudinal one. It is also possible to generate two-dimensional (2D)-disordered states for other values of the frustration by starting the simulations with 2D-disordered states. However, an understanding of the metastable states in this case does not seem possible. Therefore, and for the sake of simplicity, we focused our study only on the quasi-one-dimensional states ensuing in simulations with  $f=1/3$  and  $f=2/5$ .

In order to understand these metastable states, it proves useful to study a single domain wall. For the sake of simplicity, we assume that  $I=0$ . In the ground state, as discussed in the previous section, the current runs along the staircases. The direction of the staircase is altered by the presence of a domain wall. At the other side of it, the stair-

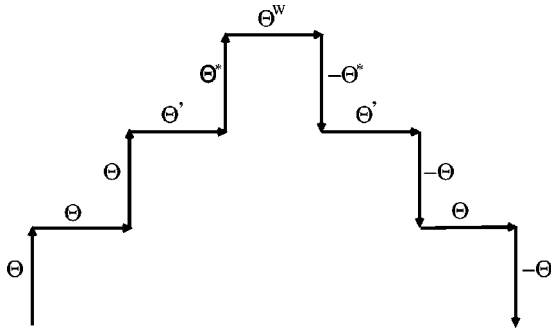


FIG. 2. Distribution of gauge-invariant phase differences around a domain wall. Notice that the horizontal gauge-invariant phase differences are symmetric across the wall, whereas the vertical gauge-invariant phase differences are antisymmetric. Sufficiently far away from the wall, the gauge-invariant phase differences are just those of the corresponding staircase states, whereas in its close vicinity they deviate from the staircase values.

case runs along the perpendicular direction, as can be seen in Fig. 2. It is natural to guess that the current continues to run along this “bent” staircase, even in the close vicinity of the domain wall. This is approximately true. Only a couple of lattice sites away from the domain wall, the gauge-invariant phase differences are just those of the ground states (corresponding to the respective symmetry of the state at the site). In the close vicinity or at the domain wall, however, there is a slight deviation from this picture, in the sense that the current is not constant along it, and deviates from the ground state value. The deviation is nevertheless not large, and amounts to only a few percent for most cases we studied, being larger at the center of the domain wall.

This picture has as consequence that at opposite sides of the domain wall the current on the vertical bonds has opposite sign, as on one side the current is going up, whereas at the other side the current is going down. On the other hand, the current on the horizontal bonds is symmetric under the inversion across the domain wall.

A given metastable state is characterized by the presence of several of these domain walls, which can be of two types, as can be seen in Fig. 3, corresponding to the two possible directions of the staircase at the left of the wall. For the sake of notation, we shall refer to them as a domain wall (DW), in which the staircase at the left of the wall is long the  $(1,1)$  direction (wherein the  $x$  direction is set equal to the direction of the injected current), and as an antidomain wall (ADW), corresponding to the staircase at the left of the wall going in the  $(1,-1)$  direction. It should be clear that a DW always appears next to an ADW, or to a boundary.

In general, the energy of a state increases the larger the number of domain walls. In this case it is unfortunately not possible to derive a general expression for the energy, which will depend not only on the number of domain walls, but also on their distribution.

These observations also provide a simple explanation for the hysteresis that is observed in the current-voltage characteristics. In fact, when starting with the ground state, just above the critical current the system is excited to a metastable state with domain walls, which has a lower critical

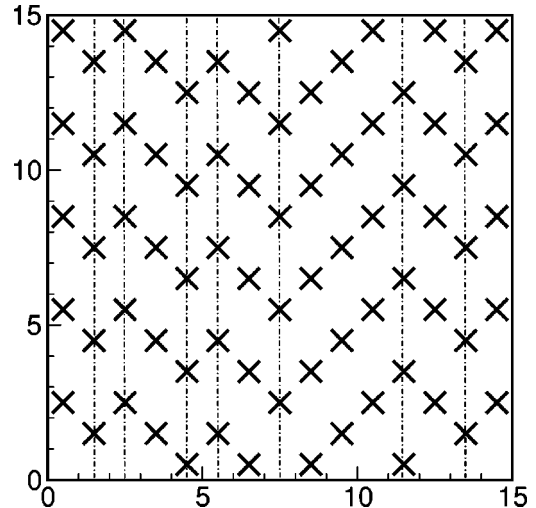


FIG. 3. Vortex configuration for a metastable state for  $f=1/3$ , produced by raising the current above its critical value, whereafter it is set equal to zero. Notice that the state is characterized by a random distribution of domain walls (signaled by the broken lines), separating regions with the symmetries of the ground state.

current than the ground state. This implies that when the current is lowered, the voltage across the array will be higher than before.

## V. CRITICAL BEHAVIOR

The critical current is the current at which the ground state becomes unstable. This is the last state to become unstable, and thus above this value of the current all states are unstable. This instability takes place through the nucleation of a domain wall next to one of the boundaries, which involves the rotation of the phases in the small region between the wall and the boundary. The ensuing state is once again unstable, and it subsequently undergoes the nucleation of a DW-ADW pair, so that the ADW appears at the site of the formerly existing domain wall, and two other domain walls appear at the two sides of it. A DW can also annihilate with a neighboring ADW. This process repeats itself, giving rise to a disordered pattern of DW's and ADW's which are constantly being created and annihilated. Moreover, due of the instability, the proliferation of the DW's seems to be favored, so that only states with a large number of DW's are observed.

The creation and annihilation of DW-ADW pairs involves a local motion of vortices. In fact, it suffices the motion of a single column of vortices for this purpose, wherefore the process can as well be understood in terms of vortex motion. On the other hand, the local vortex motion manifests itself as a sudden change in the horizontal voltage across the region where the motion is taking place. This can be seen in Fig. 4, wherein we superpose the voltage across a horizontal junction in the middle of the array with a graph depicting the motion of the vortex across the junction.

It is possible to interpret these irregular oscillations in two other ways. In terms of the phase configuration, the motion of a column of vortices necessary for the creation of a do-

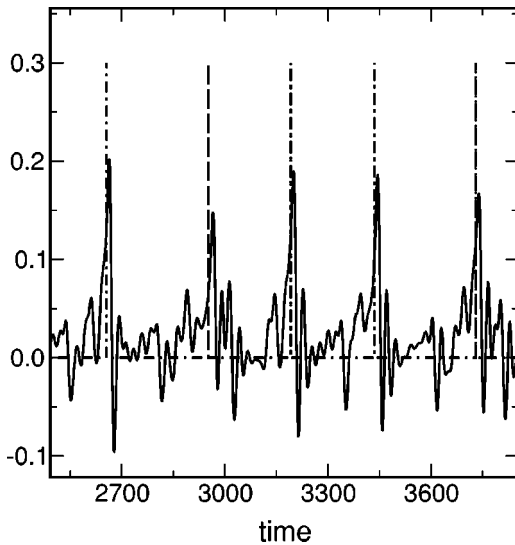


FIG. 4. Time series of the voltage across a given horizontal junction (solid) superposed to the time series of the vortex jumps (dashed). In the latter a value of zero indicates a no jump, and a finite value a jump. Notice that the spikes in the voltage correspond neatly to the spikes in the vortex jump function. While the vortex is not jumping, the voltage is much smaller, which corresponds to the period during which the system is in a given metastable state.

main wall involves the rotation of the gauge-invariant phase differences on the vertical bonds adjacent the given column by an amount equal to  $\pi$  (so that the current flowing on the vertical bonds at the two sides of the wall have the opposite signs). Thus the instability which gives rise to the vortex motion can as well be understood as an instability to the rotation of the phases by this amount. Finally, it is possible to view these irregular oscillations as a process whereby the system hops among the different subcritical metastable states (although only among those with a large number of DW's). The fact that these states correspond to subcritical metastable states (in spite of the fact that there is now a finite voltage across the junction at all times) is due to the fact that while the vortices are not jumping, the voltage across the junction is minimal, so that the system can be regarded as staying close to a metastable state during that time.

We identify the regions where vortex motion takes place as “turbulent.” These turbulentlike domains are interspeded with regular domains. They are characterized by large phase oscillations, or large voltages, whereas within the regular domains the voltages are smaller, because there the irregular oscillations correspond to oscillations around the metastable states. Within the turbulent domains, on the other hand, there are large oscillations carrying the system into other metastable states. This “turbulence” propagates itself through an “infection” process, mediated by fronts, as can be seen in Fig. 5, which is very similar to the pattern observed in other systems undergoing spatiotemporal intermittency. One could define, as well, the turbulent domains according to whether the voltage is larger than a given fraction of the maximum voltage. In fact, the two definitions provide equivalent results. A small voltage just corresponds to a small oscillation around the metastable state.

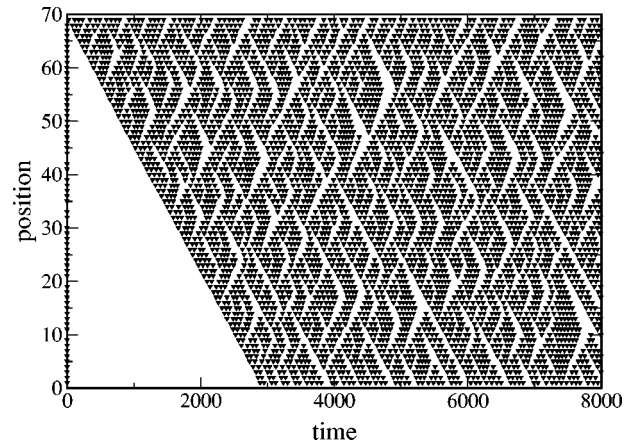


FIG. 5. Space-time distribution of vortex jumps. A black spot represents a column of vortices jumping (vortices jump simultaneously on a given column), whereas a white area represents a no jump. Thus dark areas correspond to “turbulent” regions, whereas the white areas represent the “laminar” domains. Notice the way the turbulent regions propagate within the array, which is characteristic of spatiotemporal intermittency. The simulation was done for  $f=1/3$ , and  $I=0.129$ , with an array size of  $70 \times 15$ .

The chaotic nature of the oscillations can be verified by computing the maximum Lyapunov exponent of the system, which turns out to be positive when these oscillations occur. Figure 6 displays this quantity as a function of the injected current  $I$  for  $\beta=10$ . On the other hand, decreasing the value of  $\beta$  increases the relative effect of dissipation, which leads to a suppression of the chaos (and an increase in the value of the critical current). This can be seen in Fig. 7, in which the maximum Lyapunov exponent is plotted as a function of  $\beta$  for  $I=0.129$ .

The critical nature of the oscillations can be ascertained by looking at a characteristic time scale as a function of the current. We obtained this time scale by measuring the time needed for the initial front (separating the turbulent from the

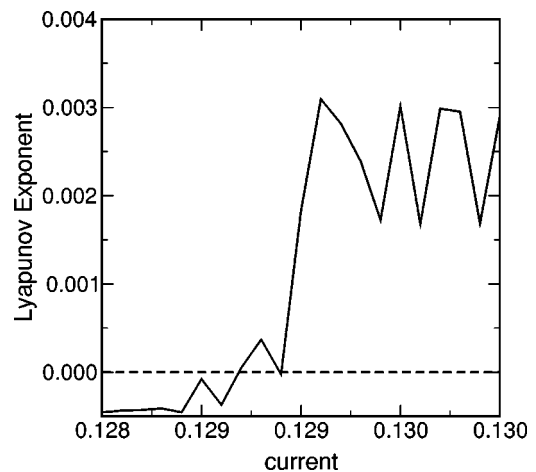


FIG. 6. Maximum Lyapunov exponent as a function of the current, for  $f=1/3$ ,  $\beta=10$  and array size  $15 \times 15$ . Notice that below a threshold the Lyapunov exponent is negative, whereas above it, it is positive, signaling the chaotic nature of the state.

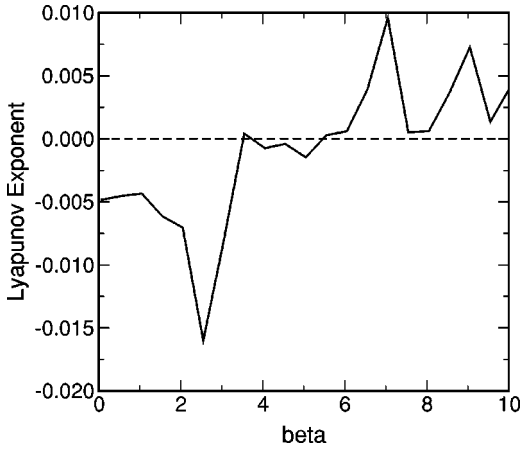


FIG. 7. Maximum Lyapunov exponent as a function of  $\beta$ , for  $f = 1/3$ ,  $I = 0.129$ , and array size  $15 \times 15$ . Notice that above a threshold the Lyapunov exponent is negative, whereas below it, it is positive, signaling the chaotic nature of the state. This is also consistent with the idea that large values of  $\beta$  suppress the chaos.

regular domains) to propagate across the entire array. This time scale is related to the lifetime of a domain wall. Our results are displayed in Fig. 8. We observe a scaling behavior for this time scale as a function of the current, which is a signature of criticality.

Another manifestation of the chaotic nature of the oscillations can be obtained by looking at the power spectrum of the voltage fluctuations, which are a measure of the collective fluctuations the system is undergoing. Figure 9 displays the power spectrum of the average voltage oscillations across the array. We observe a scaling behavior of the spectrum for large frequencies  $S(f) \sim f^\kappa$ , where  $\kappa$  is nonuniversal, and appears to depend on the case under consideration, for frequencies above the plasma and Josephson frequencies. In the uncoupled case, the plasma frequency is simply  $\omega_p = \beta^{-1/2}$ . Unfortunately in our case it is not possible to derive an analytical expression for either of the two frequencies, and since we here have a broad band of frequencies, it is in general not

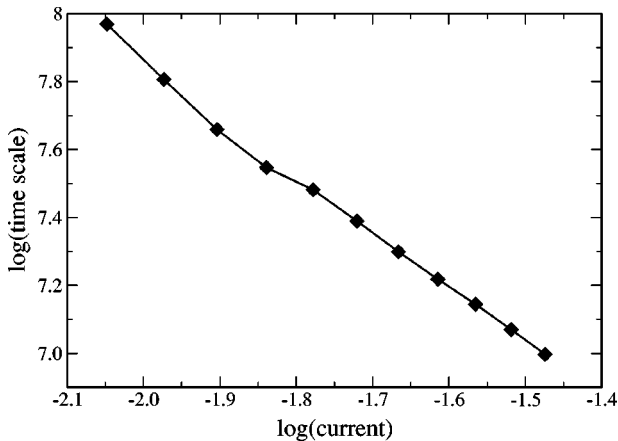


FIG. 8. Logarithmic plot of the time scale characteristic of front propagation as a function of the applied current, for  $\beta = 10$ , and array size  $70 \times 15$ . Notice the scaling relationship, characteristic of criticality  $\tau \sim (I - I_c)^{-\gamma}$ , with  $\gamma = 1.71$ .

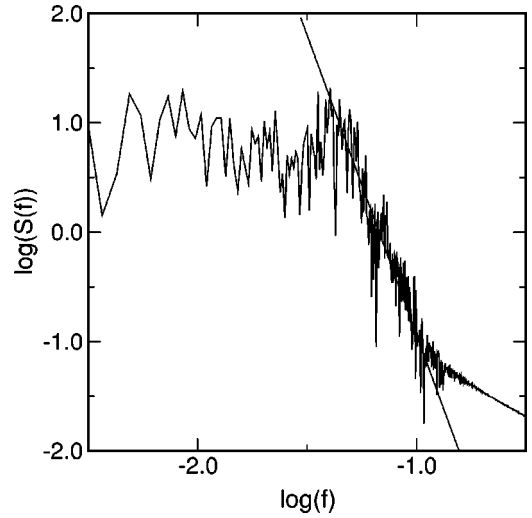


FIG. 9. Logarithmic plot of the power spectrum of the voltage fluctuations, for  $I = 0.129$ ,  $\beta = 10$ , and array size  $15 \times 15$ . Notice the scaling relationship at high frequencies  $S(f) \sim f^\kappa$ , with  $\kappa = -5.4$ .

possible to identify these two frequencies, although the rough estimate given above seems to work more or less well to define the high-frequency region.

We interpret these observations by saying that the system is undergoing spatiotemporal intermittency, which is characterized by the presence of these turbulent and regular domains, and of the  $1/f$  noise. A subcritical bifurcation may be responsible for this, as all the subcritical metastable states become unstable at the critical current. In this spatiotemporal intermittency the defects (domain walls) play a fundamental role, something which has been observed to occur in other systems.<sup>3,4</sup> We further interpret these observations in terms of the transitions among the different metastable states, which can be related to a mechanism for intermittency proposed many years ago in the case of a single Josephson junction by Ben-Jacob *et al.*,<sup>10</sup> which was on the other hand based on the more generic model of Arecchi and Lisi.<sup>11</sup> In the context of spatiotemporal intermittency, the role played by the metastable states has been emphasized within the framework of a model developed by Argentina and Coulet.<sup>12</sup>

## VI. CONCLUSIONS

We have studied the critical dynamics of a two-dimensional frustrated array of Josephson junctions, uniformly driven by a dc current. Our study has shown that at the critical current the system experiences chaotic oscillations, characterized by transitions among different subcritical metastable states. These oscillations are intermittent, since the system remains close to these states before making a transition into another state, with a different distribution of domain walls. The intermittent nature of the oscillations is shown as well by the existence of power laws relating the characteristic time scale for front propagation to the driving current, and in the high-frequency tail of the power spectrum of the voltage fluctuations.

To the best of our knowledge, this is the first theory of spatiotemporal chaos in Josephson arrays without an ac driving. Furthermore, this provides a good example of the role of multistability in the generation of spatiotemporal intermittency.

#### ACKNOWLEDGMENTS

This research was supported by the Grant No. PB96-599 from the Spanish Ministry of Science and Technology. I.M. is grateful to the same ministry for financial support.

---

<sup>1</sup>Y. Pomeau, *Physica D* **23**, 3 (1986).

<sup>2</sup>H. Chateau, in *Spontaneous Formation of Space-Time Structures and Criticality*, edited by T. Riste and D. Sherrington (Kluwer, Dordrecht, The Netherlands, 1991), pp. 273–311.

<sup>3</sup>J. D. Keeler and J. D. Farmer, *Physica D* **23**, 413 (1986).

<sup>4</sup>K. Kaneko, *Prog. Theor. Phys.* **72**, 480 (1984).

<sup>5</sup>F. Xie and H. Cerdeira, *Int. J. Bifurcation Chaos Appl. Sci. Eng.* **8**, 1713 (1998).

<sup>6</sup>F. Falo, A. R. Bishop, and P. S. Lomdahl, *Phys. Rev. B* **41**, 10 983 (1990).

<sup>7</sup>I. Marino and T. C. Halsey, *Phys. Rev. B* **50**, 6289 (1994).

<sup>8</sup>I. Marino, *Phys. Rev. B* **55**, 551 (1997).

<sup>9</sup>I. Marino, *Phys. Rev. B* **52**, 6775 (1995).

<sup>10</sup>Multistability as a source for intermittency in Josephson junctions was proposed in E. Ben-Jacob, I. Goldhirsch, and Y. Imry, *Phys. Rev. Lett.* **49**, 1599 (1982).

<sup>11</sup>The fact that intermittency may arise due to the multistability of the system was first proposed in F. T. Arecchi and F. Lisi, *Phys. Rev. Lett.* **49**, 94 (1982).

<sup>12</sup>M. Argentina and P. Coulet, *Physica A* **257**, 45 (1988).

<sup>13</sup>D. E. McCumber, *J. Appl. Phys.* **39**, 3113 (1968).

<sup>14</sup>See, for instance, *Coherence in Superconducting Networks*, Proceedings of a NATO Advanced Research Workshop, Delft, The Netherlands [*Physica B* **152**, (1988)].

<sup>15</sup>T. C. Halsey, *Phys. Rev. B* **31**, 5728 (1985).